Modeling and calibration of small-scale wind turbine blade

Anders T. Johansson[*1], **Carl-Johan Lindholm**[**], **Majid Khorsand**[*] **and Thomas Abrahamsson**[*]

[*] Chalmers University of Technology, Department of Applied Mechanics
SE-412 96 Göteborg, Sweden

[**] CCG Composites Consulting Group
SE-312 22 Laholm, Sweden

ABSTRACT

The SEM Substructuring Focus Group has chosen an Ampair 600W wind turbine to be used as a test bed in the continued efforts to further experimental and experimental-analytical substructure coupling techniques. To assess such coupling techniques, validated models of the parts, the substructures considered, play a crucial role. This paper describes the modeling, calibration and validation of a Finite Element (FE) model of a blade for the test bed turbine. Orthotropic composite material modeling is used to set up the model, which is calibrated and validated based on results from an ambitious measurement campaign including both non-destructive testing for dynamic properties and dedicated destructive tests for deduction of material properties. The measurement campaign is carefully described in the paper.

Keywords: model calibration, wind turbines, mechanical testing, vibration testing, modal analysis.

1 Introduction

IMAC XXX saw the introduction of the A600 wind turbine as a benchmark structure, as well as initial efforts in both experimental and numerical modeling, e.g. [1, 2, 3, 4]. These first efforts were predominantly focused on blade modeling. Characterization of A600 blade models has carried over to IMACXXXI, where efforts on blade modeling and calibration are reported also in [5, 6].

Likewise, the present study aims to build a high-quality Finite Element model of an A600 blade. To support the modeling, a number of material tests have been performed, ranging from thickness measurements of the blade's skin through chemical analysis for determination of the polymer materials in the blade to destructive mechanical testing for estimation of material properties. Furthermore, vibration data has been collected over a large frequency range through stepped-sine testing. From this data, frequency-domain state-space subspace (N4SID) system identification [7] is used to build a test model to which the nominal model is calibrated (updated) [8]. In a parallel study, blade variability is investigated [9]. While it is concluded in that study that the variability of the A600 blades is fairly large, this paper is concerned only with calibration to a specific blade; serial number 963.

The remainder of this paper is structured in the following way: In section 2, the material testing and Finite Element modeling of the blade is described. Section 3 describes the calibration of the model to measured data. Finally, section 4 holds concluding remarks.

[1]Corresponding Author. e-mail: **anders.t.johansson@chalmers.se**

(a) Blade cut up **(b)** Glass fibre

Fig. 1 (a) Cut blade with part labels. Parts c1 and c2 were used for compression testing of the core, 7,9 and 11 for tensile testing of the core and 13b, 13f, 14b, 14f and 15f for tensile testing of the skin, where f and b denotes front and back surface, respectively. (b) Glass fibre content of blade

2 FE model

FE modeling of the blade was performed using Siemens' pre- and postprocessor FEMAP v.10.3 with the MD NASTRAN v.2011.1 solver. The outer geometry of the blade was provided by Ampair through the SEM Substructuring Focus Group. In order to decide on the modeling strategy, a series of tests were performed to determine the material composition of the blade. Thereafter, a model was built and verified based on the stability of the first flexible eigenfrequencies upon mesh refinement.

2.1 Material testing

First, in order to identify the type of materials in the blade, shavings of the black skin and the white core (see Fig. 1a) were chemically analyzed by infrared spectroscopy and differential scanning calorimetry. The analysis indicated that both the core and the skin of the blade consisted of polypropylene (PP) [10], with signs indicating that there might be mineral material in the skin material. To verify that there was indeed mineral material in the skin and to investigate its structure, the PP resin was burned off in an oven. The resulting glass fibres, in the form woven rowing, are seen in Fig. 1b.

Table 1 Results from tensile testing. The presented quantities are: Tested specimen identification code, thickness t and estimated modulus E (directional). For definition of the different specimens, see Fig. 1a

Core			Skin		
ID	t [mm]	E [MPa]	ID	t [mm]	E [MPa]
7	6.0	1590.4	13b	2.7	6432.9
9	6.0	1374.5	13f	2.9	7732.9
11	6.0	2270.7	14b	2.8	8510.9
			14f	2.9	10237.7
			15f	3.0	3280.6
Mean	6.0	1745.2	Mean	2.86	7239.0
Stdev	0.0	467.7	Stdev	0.11	2606.3

Thus concluding that the blade consists of a skin with a woven glass fibre in a PP resin set on a PP core, some educated guesses on the material data for FE modeling could be formed. To substantiate the material parameters further, mechanical testing of the coupons cut out of the blade according to Fig. 1a was performed. The tensile stiffness of the coupons was evaluated by tensile testing. The results are shown in Table 1. Because the blade does not present any planar surfaces, the

preparation of uniform coupons for the skin presented some difficulties. The thickness of the samples was also subject to some variation, both between samples and within the same sample. This serves as an explanation for the large spread in data seen for the skin material.
In addition to the tensile testing, compressive tests of the core was performed (on part c1 and c2). The results of the two tests had a mean value of about 800MPa; however, experience has shown that bulk data estimates from this type of testing are to be viewed as lower limits. Since the compression coupons also were very small out of necessity, the results were deemed less reliable.
The compression coupons were also used for estimation of the core material density, found to be 818kg/m^3. The weight of the full blade was 798.4g.

2.2 Modeling

Drawing on the results from the testing stage, the FE model was built as a laminate skin on an isotropic core. The core was modeled by linear four-noded tetrahedral elements (CTETRA) using an isotropic material model with the mean measured Young's modulus, E =1745MPa, and an estimated Poisson's ratio of $\nu = 0.3$ and density 818kg/m^3.
The skin was modeled predominantly by four-noded rectangular plate elements (CQUAD4), with a few triangular (CTRIA). Common practice to model glass-reinforced plastic materials is to use composite shell elements. Because of this, the measured values are recalculated to an equivalent unidirectional ply. This also makes it easier to estimate the shear properties - shear in a unidirectional ply can be estimated based on the shear modulus of the isotropic resin property, thus $G = E/2(1+\nu)$.The material model of the skin was prepared using the built in laminate theory of FEMAP. The layup consists of four layers, each 7mm thick (to yield a total thickness of 2.8mm), stacked in the order $0^\circ - 90^\circ - 0^\circ - 90^\circ$. Compare this to the weave of Fig. 1b; four layers are used since experience has shown that it represents a weave more accurately.
The orthotropic material model used for the layers was prepared to match the measured stiffness; the Young's modulus in the direction perpendicular to the fibre direction was set to that of PP at E_2 =1745MPa, whereas in the fibre direction the stiffness was estimated to E_1 =14.5GPa. The shear modulus in the different directions were set to 700MPa in all three directions and $\nu_{12} = 0.3$. This ensures a bulk stiffness of 7228MPa in the $0^\circ - 90^\circ$-directions of the plane, corresponding to the measured mean. For details, confer [11].
The skin of the model was furthermore modeled using an offset to ensure that the outer surfaces of the geometry are also the outer surfaces of the model. This will however mean that there is an overlap of skin and core material in the skin. To match the measured weight of the model, the density of the skin was tuned in at 272kg/m^3, yielding a model weight of 798.6g, differing by only 0.2g from the measured value. Because of the overlap, the skin material density estimate arrived at in this manner is 1090kg/m^3.
In this study, all computations have been eigensolutions made in free-free conditions. Thus, six rigid body modes are included in each result set; these will however not be presented. When the first mode is referred, the first flexible mode is implied.

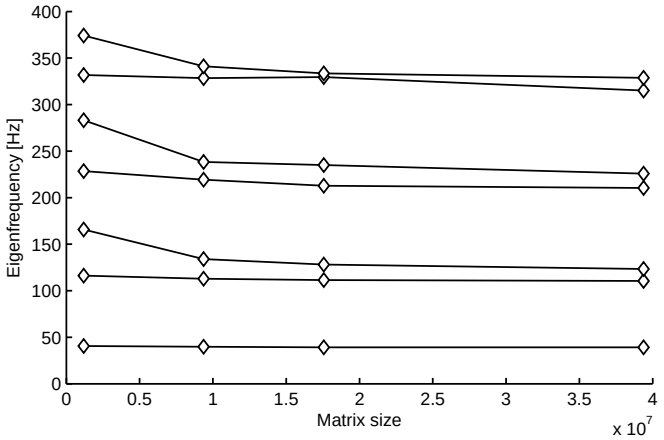

Fig. 2 Verification of mesh size. The first seven eigenfrequencies analyzed using four different models. The mesh was deemed converged after one refinement. Note that the frequencies in this figure do not correspond to the nominal values.

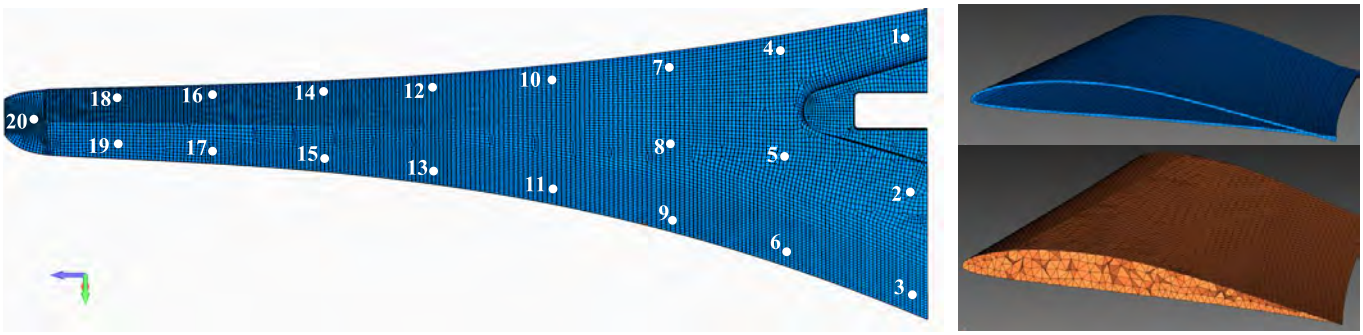

(a) Finite element model of blade with measurement set highlighted **(b)** Close up of skin and core mesh

Fig. 3 Finite Element model, dynamic measurement set and skin and core mesh

2.3 Verification

To ensure convergence of the mesh, a convergence analysis of the first seven eigenfrequencies with respect to four models of increasing order was performed. The solution times varied from a few seconds to hours from coarsest to finest mesh. The results of the convergence study is shown in figure 2. Note that at the time of the convergence analysis, the material data was not fully analysed and so the eigenvalues do not correspond to those of the nominal model. It was decided that the convergence was good enough for the second coarsest model; this model is used henceforth. It consists of 317390 nodes and 209714 elements, of which 25 347 are linear laminate plates and the remaining 184367 are solid tetras. The model is seen in figure 3.

3 Model calibration

This section describes a model calibration campaign to improve the predictive quality of the A600 blade model over a large frequency range.

3.1 Vibration measurements

To validate the blade model described in the previous section, a stepped sine test was performed in the frequency range from 30 to 900Hz with 0.2Hz increments, exciting 12 of the first flexible modes of the system. 20 accelerometers were used to record the accelerance of the system in the direction perpendicular to the blade at the same locations used in [4, 9]. The measurement set is depicted in Fig. 3a. The system was excited perpendicular to the blade surface at node 1, and eigenvalues and eigenvectors were extracted from the data by identifying a linear time invariant model of the proper order using frequency-domain system identification by the system identification toolbox in Matlab [7]. By using the relation $A(\omega) = j\omega Y(\omega)$, where A is the accelerance and Y the mobility, the system identification could be carried out on mobility data. This ensures that the high-frequency modes are comparatively less influential on the response of the system.

3.2 Initial correlation

A comparison of the measured eigenvalues and eigenvectors to the nominal FE modes was conducted, seen in Table 2 and Fig. 4a. The results show a fairly large frequency deviation, with a maximum of 5.5% relative error for the first five flexible modes, where the MAC correlation between measured and analytical eigenvectors is good. Beyond the fifth mode, no modes can be said to correlate well for the nominal model. Thus, the model needs calibration.

3.3 Calibration

There are many different techniques for model calibration, many of them described in the standard textbook by Friswell and Mottershead [8]. In this study, the linear error in eigenfrequency has been used as the cost function, calculated as:

$$J(\boldsymbol{\theta}) = \boldsymbol{\varepsilon}(\boldsymbol{\theta})^T \boldsymbol{\varepsilon}(\boldsymbol{\theta}) \tag{1}$$

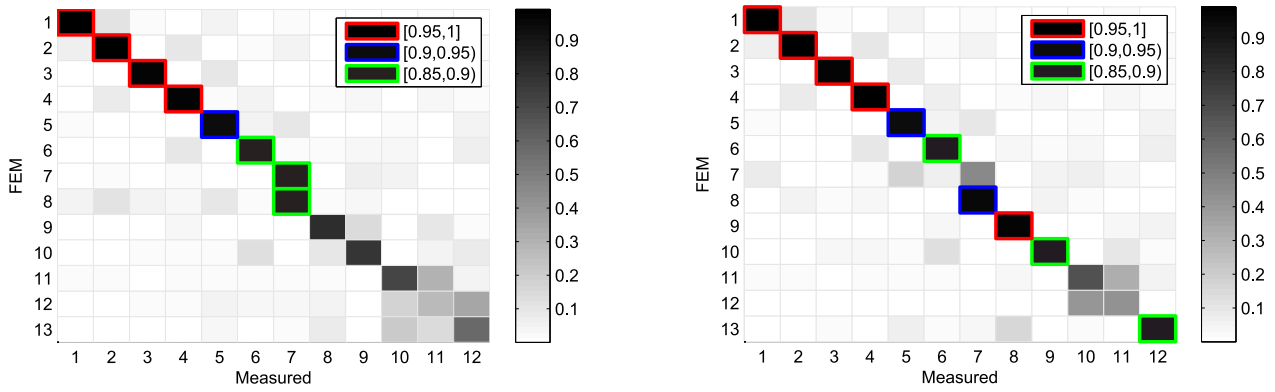

(a) Nominal model - measurement

(b) Calibrated model - measurement

Fig. 4 MAC correlation plots. (a) MAC matrix for correlation between nominal model modes and measurement modes. (b) MAC matrix for correlation between calibrated model modes and measurement modes

where

$$\boldsymbol{\varepsilon}(\boldsymbol{\theta}) = \begin{bmatrix} \vdots \\ f_i^{Meas} - f_j(\boldsymbol{\theta})^{FEM} \\ \vdots \end{bmatrix} \tag{2}$$

Here, f_i^{Meas} and f_j^{FEM} are the i:th measured and j:th Finite Element eigenfrequencies in Hz, respectively. i and j are matched indices, resulting from a mode pairing scheme aimed at ensuring that the eigenfrequency of the FE mode which most accurately represents a given measured mode is compared to that mode. Mode pairing is described further in [12]. Because of the poor correlation beyond the fifth mode, it was decided that only the first five modes were to be used in the model calibration scheme. The argument $(\boldsymbol{\theta})$ is used to indicate dependence of the updating parameters.
Because of the large spread in the static measurements, it was found that the bulk data parameters were suitable for updating. Thus, a parameter vector consisting of the six main bulk data entries was set up, i.e:

$$\boldsymbol{\theta} = \ln[E_{1,skin}\ E_{2,skin}\ G_{12,skin}\ G_{1z,skin}\ G_{2z,skin}\ E_{core}]^T \tag{3}$$

Where the natural logarithm was used in the parameter definitions to contract the parameter space. A single starting point was generated, from the parameters of the nominal model described above. Constraints were introduced approximating the level of uncertainty in the modeling, and the Active Set algorithm in Matlab's optimization toolbox [13] was used to find a local minima of the cost function. Gradients were approximated numerically by Matlab.
The resulting parameters are shown in Table 3. No constraints were active for the final result. The resulting eigenfrequencies and MAC correlations can be seen in Table 2 and Fig. 4b, respectively.

3.4 Validation

Since the model was calibrated using only the first five eigenfrequencies as parameters, seven more eigenfrequencies are available for validation purposes. After updating, it is found that all of the modes have a relative error below 3% except for the highest mode. In a parallel study, it was shown that the coefficient of variation describing the variability between blades was also at around 3%. Since the MAC correlation of eigenvectors has also improved dramatically after calibration, the model can be deemed validated.
If one is very generous in defining correlation (as MAC>85%), three modes remain uncorrelated, with FE mode number 7 standing out the most in that it seemingly does not have a measurement counterpart at all. It may not be fully clear in Fig. 5g, but this is an edge-wise bending mode, and so the main deflection of the mode is perpendicular to both the sensing and the actuating of the measurements, and hence it is both unobservable and uncontrollable. Thus, this is an effect of the measurement setup rather than the model. Mode 10, Fig. 5j, is a mode dominated mainly by deflection in the weak corner of the blade's base, and Mode 11, Fig. 5k, seems to have vibrational node lines at about the same length-direction intervals as we are sensing, making it largely unobservable and sensitive to slight misalignments of the FE output to the Measurement positions.
Taking all these factors into account, the model presented in this study seems to be a good working model of an Ampair 600W blade.

(a) Mode 1, 45.2Hz

(b) Mode 2, 128.9Hz

(c) Mode 3, 188.1Hz

(d) Mode 4, 250.2Hz

(e) Mode 5, 326.1Hz

(f) Mode 6, 405Hz

(g) Mode 7, 452.2Hz

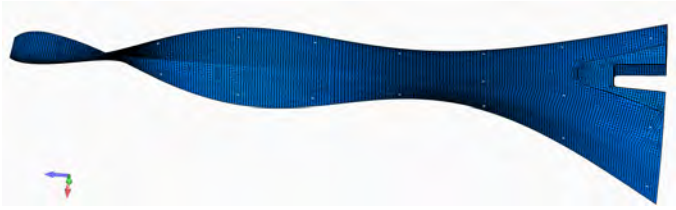

(h) Mode 8, 474.2Hz

(i) Mode 9, 584.5Hz

(j) Mode 10, 631.2Hz

(k) Mode 11, 734.7Hz

(l) Mode 12, 779.0Hz

(m) Mode 13, 823.4Hz

Fig. 5 Flexible vibrational modes of calibrated FE model.

Table 2 Comparison between measured and Finite Element eigenfrequencies in [Hz]

	Frequency comparison [Hz]			Relative comparison [%]	
	Measured	FEM Nominal	FEM Calibrated	Meas.-FEM Nom.	Meas.-FEM Cal.
Mode 1	46.5	48.1	45.2	3.5	2.7
Mode 2	129.4	136.5	128.9	5.5	0.4
Mode 3	191.7	181.9	188.1	5.1	1.8
Mode 4	250.7	264.1	250.2	5.3	0.2
Mode 5	324.0	317.7	326.1	2.0	0.7
Mode 6	404.5	426.4	405.0	5.4	0.1
Mode 7	- -	455.4	452.2	- -	- -
Mode 8	481.3	476.2	474.2	1.1	1.5
Mode 9	576.7	609.7	584.5	5.7	1.4
Mode 10	647.6	622.0	631.2	4.0	2.5
Mode 11	750.4	746.2	734.7	0.6	2.1
Mode 12	769.1	797.0	779.0	3.6	1.3
Mode 13	857.6	831.2	823.4	3.1	4.0

Table 3 Comparison between nominal and calibrated material parameter values

	$E_{1,skin}$	$E_{2,skin}$	$G_{12,skin}$	$G_{1z,skin}$	$G_{2z,skin}$	E_{core}	[GPa]
Nominal Value	14.5	1.75	0.7	0.7	0.7	1.75	
Calibrated Value	11.6	2.84	0.90	0.72	0.72	1.67	

4 Conclusions

This paper presents a FE model of Ampair A600W wind turbine blades. The model is built using laminate theory in the skin and linear isotropic material modeling in the core. Several tests were performed to identify and characterize the materials of the blade. The model was successfully verified, calibrated and validated based on dynamic testing in the frequency range from 30 to 900Hz.

Using the built-in laminate theory in FEMAP to compute the stiffness parameters of the skin layup based on the calibrated parameters results in 6772MPa, which is well within the standard deviation of the tensile testing results at 7239.0 ± 2606.3MPa. Likewise, the calibrated core stiffness was 1666MPa which is within the bound at 1745.2 ± 467.7MPa.

After calibration, all eigenfrequencies but one are within 3% of the measured values and the MAC matrix is diagonal-heavy. The relative lack of correlation for some modes can however be explained in terms of observability and controllability.

5 Acknowledgements

The authors would like to acknowledge Jerry Stigsson and Håkan Lindqvist at DIAB AB for their respective contributions to the laboratory testing of this paper. The FE modeling of the paper has been assisted by Johan Hedlund at CCG Composites Consulting Group.

References

[1] Mayes, R., *An Introduction to the SEM Substructures Focus Group Test Bed The Ampair 600 Wind Turbine*, in Proceedings of the SEM IMAC XXX Conference Jan. 30 - Feb. 2, 2012, Jacksonville, FL USA, 2012.

[2] Mayes, R., *Wind Turbine Experimental Dynamic Substructure Development*, in Proceedings of the SEM IMAC XXX Conference Jan. 30 - Feb. 2, 2012, Jacksonville, FL USA, 2012.

[3] Nurbhai, M.S., Macknelly, D.J., *Modal Assessment of Wind Turbine Blade in Preparation of Experimental Substructuring*, in Proceedings of the SEM IMAC XXX Conference Jan. 30 - Feb. 2, 2012, Jacksonville, FL USA, 2012.

[4] Harvie, J., Avitabile, P., *Comparison of Some Wind Turbine Blade Tests in Various Configurations*, in Proceedings of the SEM IMAC XXX Conference Jan. 30 - Feb. 2, 2012, Jacksonville, FL USA, 2012.

[5] Linderholt, A., Chen, Y.C., *Model Calibration of an A600 Wind Turbine Blade*, in Proceedings of the SEM IMAC XXXI Conference Feb. 11-14, 2013, Los Angeles, CA USA, 2013.

[6] Nurbhai, M., Macknelly, D., *Dynamic Structuring Turbine Blade FE Model Update and Correlation With Test*, in Proceedings of the SEM IMAC XXXI Conference Feb. 11-14, 2013, Los Angeles, CA USA, 2013.

[7] McKelvey, T., Akcay, H. and Ljung, L., Subspace-based multivariable system identification from frequency response data, IEEE Transactions on Automatic Control, 41, 1996, 960-979.

[8] Friswell, M. I., Mottershead J. E., Finite Element Model Updating in Structural Dynamics, Kluwer Academic Publishers, Dordrecht, 1995.

[9] Gibanica, M. *et. al*, *Spread in modal data obtained from wind turbine blade testing*, in Proceedings of the SEM IMAC XXXI Conference Feb. 11-14, 2013, Los Angeles, CA USA, 2013.

[10] Brydson, J.A., Plastics Materials, Referex Engineering, Elsevier Science, 1999.

[11] Zenkert, D., The Handbook of Sandwich Construction, EMAS Ltd., 1997.

[12] Möller, P, Friberg, O., An approach to the mode pairing problem, Mechanical Systems and Signal Processing, 12, 1998, pp. 515-523.

[13] Gill, P. E. *et al*, Procedures for Optimization Problems with a Mixture of Bounds and General Linear Constraints, ACM Trans. Math. Software, Vol. 10, pp. 282-298. 1984.